2009

# Drag Measurement of a Sphere in Helium II

Ali Hemmati

FLORIDA STATE UNIVERSITY

FAMU–FSU COLLEGE OF ENGINEERING

# DRAG MEASUREMENT OF A SPHERE IN HELIUM II

By

ALI HEMMATI

A Thesis submitted to the Department of
Mechanical Engineering
in partial fulfillment of the
requirements for the degree of
Master of Science

Degree Awarded:
Spring Semester, 2009

The members of the Committee approve the Thesis of Ali Hemmati defended on March 27, 2009.

Steven Van Sciver
Professor Directing Thesis

Chiang Shih
Committee Member

Eric Hellstrom
Committee Member

Approved:

Chiang Shih, Chair, Department of Mechanical Engineering

Ching-Jen Chen, Dean, FAMU–FSU College of Engineering

The Graduate School has verified and approved the above named committee members.

# ACKNOWLEDGEMENTS

I would like to thank cryolab group for their help and support, and also would like to thank my advisor Dr. Steven Van Sciver for his unlimited support and help. I would like to thank the committee members Dr. Chiang Shih and Dr. Eric Hellstrom for their suggestions and willingness to help.

I like to thank Kenneth Pickard for helping with the winding of magnets, and Russell Wood for helping with the wiring. Tom Dusek did the fantastic glass work and helped to build the channel. I also like to thank Dr. Ting Xu for his suggestions with the cross-correlation codes, and Dr. Sylvie Fuzier for helping with the visualization.

This work is supported by the National Science Foundation under grant CTS-0729972

# TABLE OF CONTENTS

# LIST OF FIGURES

# ABSTRACT

An apparatus to measure the drag on an oscillating 3 mm niobium sphere in superfluid helium has been built and tested. A Nb-Ti superconducting solenoid is used to suspend the niobium sphere; meanwhile a similar superconducting quadruple magnet centers and helps to stabilize the ball at one location in the flow channel. The niobium sphere is levitated by the superconducting magnetic suspension system; then the oscillation is obtained by dropping the ball from one equilibrium point to a lower equilibrium point via reducing the magnetic field. The sphere's oscillation is then recorded with a high-speed CCD camera. The velocity of the sphere is then obtained by comparing the images captured and the distance the sphere has moved with time. Drag force is calculated through its relation to the maximum velocity decay rate. The sphere is contained within a closed end channel that allows measurements in liquid or gaseous helium and vacuum.

# CHAPTER 1

# INTRODUCTION

## 1.1 Drag Coefficient

The force of drag as an object moves through a fluid has been known for many years. It was used to sail ships, in wars it was used to guide arrows, and is the reason for man to be able to fly. In many of these scenarios, the people who took advantage or were disadvantaged by it, may or may not have known the reason behind this powerful force. Archimedes was the first person who discovered buoyancy, and so the law of buoyancy is called Archimedes' principle, which determines the mass of an object submerged in a fluid by determining the amount of fluid displaced. By using Newton's laws we should be able to setup a scenario in which the acceleration of an object can be determined. For example, if a submarine is going under water in a non-constant rate, how long would it take for the submarine to reach a certain depth? By only using the force equation we will not be able to answer such a question. The density and the viscosity of ocean water play an important role in answering such a question. The shape of the submarine plays an additional factor in determining the time for it to reach certain depth.

Drag force is an opposing force that the fluid exerts on an object in a direction opposite to its motion. To determine the drag force, we must define the drag coefficient, which is a non-dimensional value that determines the resistance of a body in a fluid based upon the body's shape and structure. The drag coefficient is defined by the following equation,

$$C_D = \frac{F_D}{\frac{1}{2}\rho A v^2} \tag{1.1}$$

where $\rho$ is fluid density, $v$ is fluid velocity, $A$ can differ based upon object but for sphere is the frontal area, and $F_D$ is the drag force.

The drag coefficient is the parameter that characterizes the behavior of the drag force

on a body. There are numerous experiments that have been done to determine the drag coefficient of many different shapes in terms of Reynolds number; where Reynolds number is defined as,

$$Re = \frac{\rho v D}{\mu} \tag{1.2}$$

where $v$ is fluid velocity, $D$ is effective diameter, and $\mu$ is viscosity. Reporting drag versus Reynolds number is a way to scale all the measurements of drag and makes it simple to compare different drag measurements independent of the medium.

The determination of drag coefficient plays an extremely important role in design of airplanes, automobiles, boats, and many more vehicles. For certain applications such as jet airplanes and extremely high speed vehicles that go into very high Reynolds numbers, full scale testing can become difficult and costly. Liquid helium has kinematic viscosity much smaller than air (nearly three orders of magnitude); therefore, testing in helium for the same or smaller scale model problems can provide solutions to high Reynolds number problems[2].

A very well known shape that has always captured the interest of scientists is a sphere. It has a simple shape with an easy to calculate cross sectional area and volume. Also, in laminar flow there is an analytic solution for the drag coefficient. The drag on a sphere has been studied extensively in classical fluids such as water and air[3]. Figure 1.1 displays normal behavior for a drag coefficient of sphere versus Reynolds number. A Curve fit equation is given by White[4] that offers a fit for drag on a sphere in laminar regime, before the "drag crisis" for Reynolds number range of $0 \leq Re \leq 2 \times 10^5$ and is given as,

$$C_D \approx \frac{24}{Re} + \frac{6}{1+\sqrt{Re}} + 0.4 \tag{1.3}$$

Equation 1.3 has accuracy of $\pm 10$ %. In the crisis regime the wake behind the sphere thinens due to turbulent boundary layer, and so the drag is reduced. In this experiment, we are interested in drag on a sphere in He II.

## 1.2 He II

Helium has the lowest critical point of all fluids, $T_c = 5.2$ K, and $P_c = 0.226$ MPa. According to the phase diagram in figure 1.2, helium can exist in two completely different states. Also, since helium does not solidify at low temperatures without an external pressure of more than 2.5 MPa it has no triple point He I behaves as a classical fluid, and it has classical properties

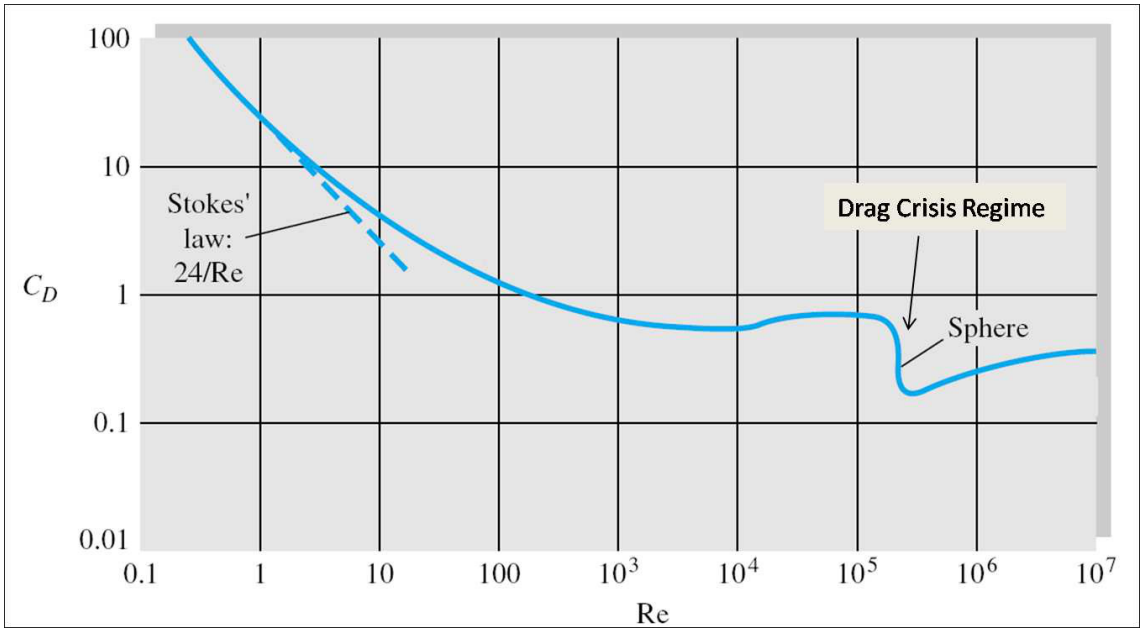


Figure 1.1: Sphere drag coefficient vs. Reynolds number for classical fluid[1]

until the transition to He II. The line that separates these two states is called the $\lambda$-line. The $\lambda$-point at which transition occurs is at 2.176 K at saturated vapor pressure, and the transition temperature continues to decrease as pressure is increased. Coexistence of He I and He II in equilibrium conditions is not possible.

He II is classified as quantum fluid because it has properties that can only be understood in terms of quantum mechanics. For example, considering transport properties, He II has extremely small viscosity and very high thermal conductivity, many orders of magnitude larger than classical liquids. He II cannot nucleate bubbles in the bulk. This is due to He II's very high thermal conductivity that does not allow significant thermal excursions to occur in the bulk of the liquid, and the heat is transported to the surface by a conduction-like mechanism.

### 1.2.1 Two fluid model

As described before, He II has exceptional and non-classical like fluid behavior. One of these properties is the viscosity of the fluid. Depending on the method performed to measure this property, He II can show different values for its viscosity. These two methods are 1) a

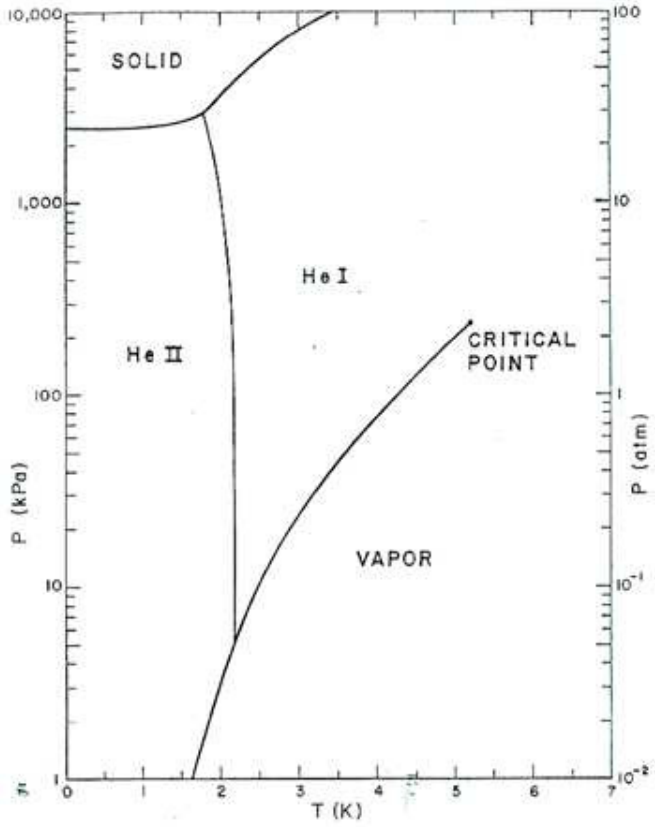


Figure 1.2: Helium phase diagram

rotating disk, and 2) laminar flow through a narrow channel. For normal fluids, including He I, both methods yield almost same value for the viscosity. However, in He II the viscosity yields a finite value for rotating disk and almost zero for flow through channel experiment. This behavior can be explained by a model Tisza developed in 1938 later refined by Landau (1941)[5].

The two-fluid model can be thought as two interpenetrating fluids, normal fluid and superfluid, which have temperature dependent densities and are fully miscible. These two components describe the dynamics of He II under temperature or pressure gradient. The normal fluid is assumed to behave as a classical fluid and have a density $\rho_n$, viscosity $\mu_n$, and entropy $s_n$. Although, the superfluid part has a density $\rho_s$, it has zero viscosity, and

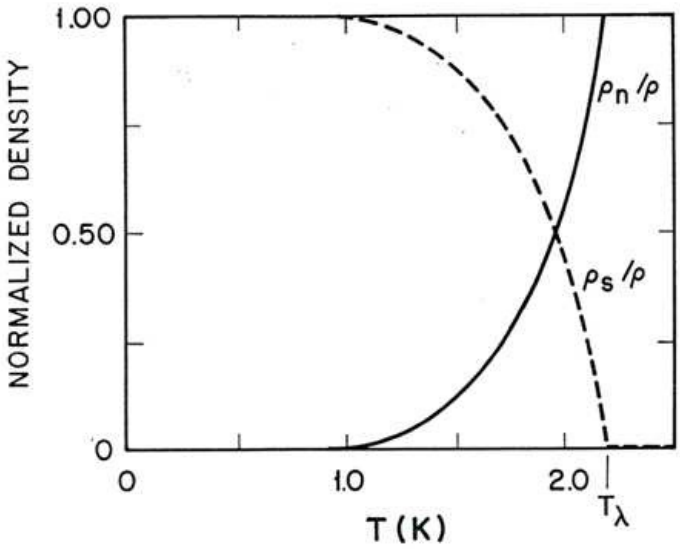


Figure 1.3: Ratio of normal fluid density and superfluid density in He II

zero entropy. Therefore, all the entropy in He II is carried by the normal fluid component. Then, average heat current can be given as,

$$q = \rho s T \langle v_n \rangle \tag{1.4}$$

where, $v_n$ is normal fluid velocity. The total density of He II is the addition of densities of both normal fluid and superfluid components and is given as,

$$\rho = \rho_n + \rho_s \tag{1.5}$$

with the momentum of the fluid given as,

$$\rho v = \rho_s v_s + \rho_n v_n \tag{1.6}$$

In laminar flow it can be shown that effective thermal conductivity, $k_{eff}$, of He II is strongly dependent upon diameter of channel and temperature.

$$k_{eff} \sim d^2 T^{12} \tag{1.7}$$

### 1.2.2 Turbulence in He II

Equation 1.7 is only accurate up to a certain point. There exists a critical velocity above which, He II does not behave ideally as described above. This has been proven by

experimental measurements. Turbulence in normal fluid component is classical turbulence and it occurs at Reynolds number greater than about 1200. This Reynolds number is obtained by using normal fluid density and viscosity. Turbulence in superfluid helium is caused by formation of quantized vortex lines. There exist some experiments that are capable of visualizing these vortex lines. These experiments have, to a certain point, been able to explain the contradictions seen between two fluid model and experiments[6].

The superfluid critical velocity, $v_{sc}$, can only be explained by quantum mechanics. Study of $v_{sc}$ has not been greatly successful, and it is experimentally determined to be given as (in cgs inits (cm)),

$$v_{sc} \cong d^{-\frac{1}{4}} \tag{1.8}$$

# CHAPTER 2

# BACKGROUND

There has always been the question of whether the same physical fluid dynamic properties that apply to classical fluids such as He I can be applied to He II. As described previously, once liquid helium is below the $\lambda$-line, the two fluid model governs the dynamics of the fluid; therefore, an important question is whether classical properties such as finite viscosity in liquids can be assumed any further? One of the properties of interest is the behavior of drag on a sphere, which in classical fluids has been well studied. In classical fluids, there are correlations that can predict the drag coefficient on a sphere for Reynolds number $Re < 10^5$ with an average of 10% error and is presented in equation 1.3. An important goal would be to develope a similar condition to estimate the drag coefficient for He II.

The drag on a sphere in He II has only been studied by a few researchers[7]$^-$[12]. Most of these studies have involved either using an external device attached to the sphere to suspend it in the flow field, or simply releasing the sphere to fall freely at its terminal velocity. Smith *et al* studied the drag on a 10 mm diameter sphere suspended in a 40 mm channel by small capillary tubes that also acted as pressure taps. They used the pressure distribution over the sphere to compute the drag coefficient. Smith[7](1998) in which he and his colleagues were able to observe drag crisis in the range of Reynolds number $10^5 \leq Re \leq 10^6$ on the sphere in He I and He II and saw no significant difference between the two measurements. An example of some of their drag measurements is shown in figure 2.1

Dropping a sphere and measuring its terminal velocity and then finding the drag coefficient is a method used by Laing[8] et al (1960) . They repeated the experiment in different liquids other than He II, and received similar results. Some of the results that they have obtained are shown in figure 2.2. These results are not very suitable due to large error they acquire when determining terminal velocity of the sphere. Most of the values they have

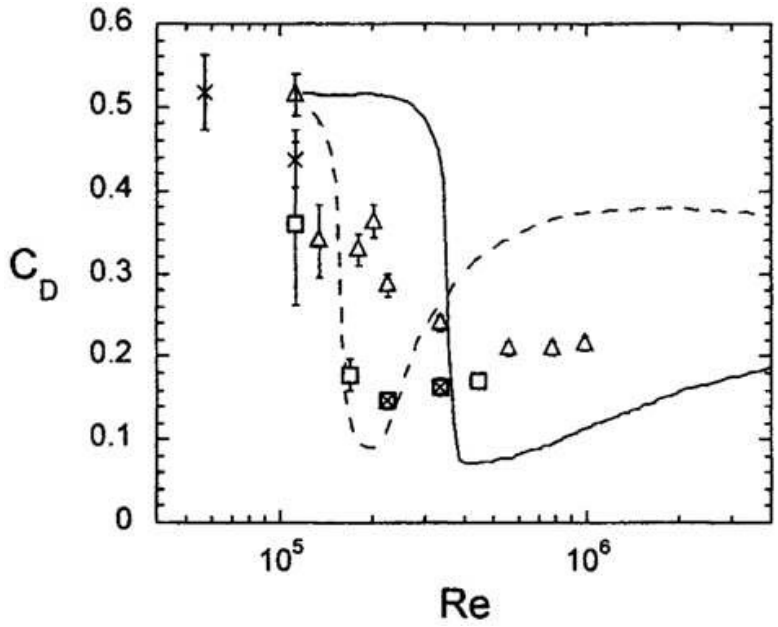


Figure 2.1: Drag coefficient as a function of Reynolds number. The open squares and crosses correspond to temperatures 2.54 K and 4.2 K, respectively. The triangles were recorded at 1.8 K. The full curve is the accepted classical result and the dashed curve shows the effect of a surface roughness of 0.0015. After Smith[7] et al (1998).

obtained in classical fluids do not match other experiments done in classical fluid.

Drag measurement on an oscillating object can produce slightly different result than steady drag measurement. The drag on a sphere moving with some velocity, which is dependent on time, is different than the drag on a steady sphere[9].

Shoepe and his colleagues[10] performed a drag measurement on an oscillating magnetic sphere of diameter of about 100 $\mu m$ suspended between niobium plates shown in figure 2.3. They report a drag coefficient similar to that of classical fluid in the turbulent regime of He II, although the main experiment was conducted at 1 K and below, and also in laminar regime. Shoepe *et al* obtained for these ranges of temperatures and Reynolds numbers, behavior that does not coincide with that of classical fluids.

Overall, experimental results that have reported the drag coefficient in He II in turbulent regimes or for that matter friction factor measurements in pipe flow have displayed classical-like behavior. For the most part, this observation is based on the argument that at higher velocities both normal and superfluid components are in the turbulent state and in this state

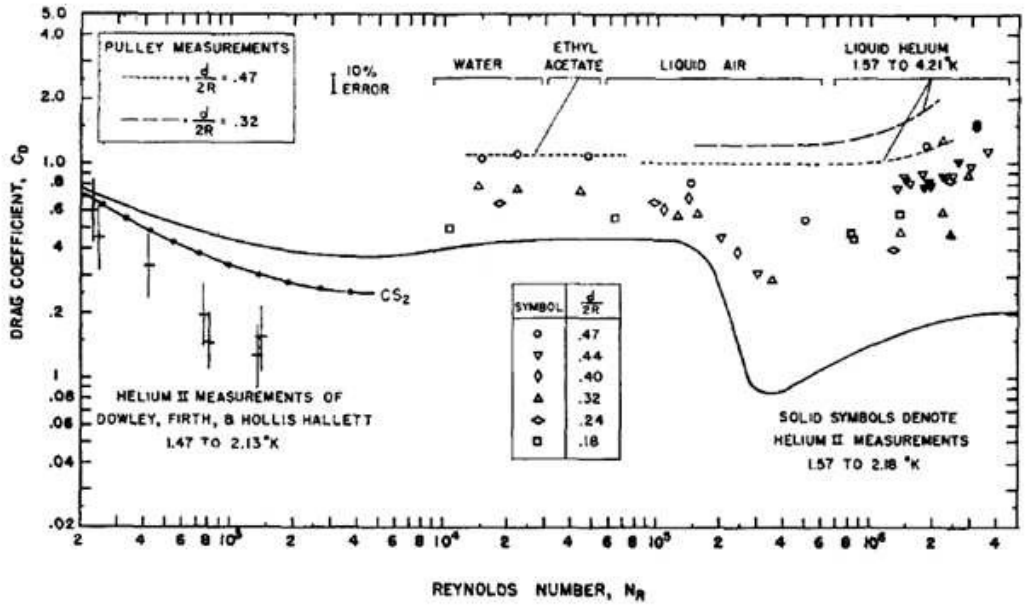


Figure 2.2: Laing and Rorschach[8] result for drag on a sphere versus Reynolds number

both components couple and this coupling effect make the two fluids move together as if they were a classical fluid.

The present experiment is a simpler version of a previous design for a diamagnetic sphere suspension system for liquid helium[11] suggested by Smith et al. Although the apparatus in the previous design was horizontal and no visualization was suggested, it provides some detail about what kind of magnet, size of sphere, and channel to use to obtain optimum results. In Smith's design, the drag on a sphere is measured by using pick up coils to detect the distance that the diamagnetic sphere will move under the influence of drag. The suggested system was for a steady drag measurement.

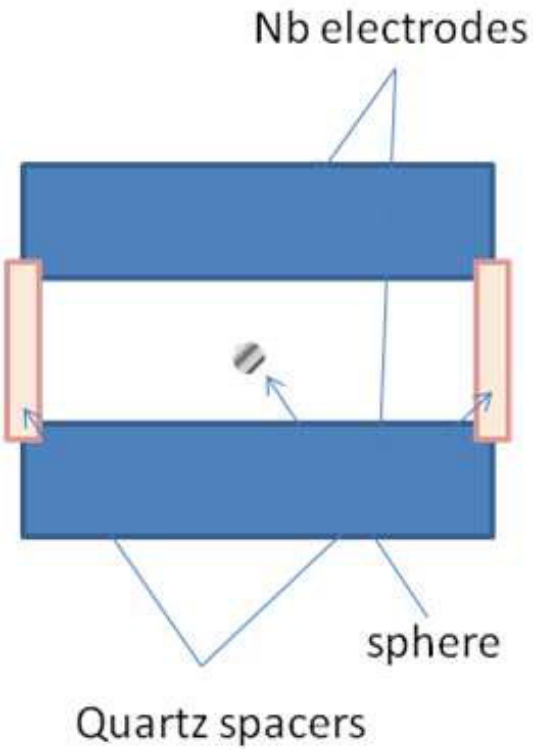


Figure 2.3: Schematic of what Niemetz and Shoepe[10] used to oscillate the 1 pC charged ferromagnetic 100 $\mu m$ size sphere

# CHAPTER 3

# EXPERIMENTAL APPARATUS & TECHNIQUE

The present experiment is design to measure the damping of an oscillating sphere in low temperature helium. To achieve this measurement, it is both necessary to have a method of suspending the sphere in the flow field and measuring its velocity. We suspend a diamagnetic sphere in a magnetic trap and measure its velocity using visualization techniques.

The sphere is made of pure niobium, which becomes superconducting below 9.2 K and is perfectly diamagnetic below $B_{c1} \simeq 0.25$ T, so it can be levitated by an external magnetic field. Once enough force by the magnetic field is provided, the sphere rises to a certain level and can oscillate within a magnetic trap. Then, the oscillation is recorded by a digital camera and analyzed frame by frame to track the velocity of the sphere. Once the velocity is obtained, it can be matched against its theoretical value for a certain drag coefficient.

The main objective of this experiment is to measure the drag force on a niobium sphere in He II. Our technique involves suspending a perfectly diamagnetic sphere in a magnetic trap. This method has an advantage in that the sphere is not in contact with any physical objects that can create their own drag and interfere with the measurement. Moreover, this technique provides a unique way to look at how spheres oscillate and move in low temperature helium, gas or liquid.

Since the magnetic field changes at every point in the channel, the disadvantage of a magnetic suspension system are the complications with changing magnetic forces and effect of these forces on an oscillating diamagnetic sphere. In the following section, we describe how these issues have been resolved in the present case.

There are four major components that make up the experimental system. They are: a) The launching superconducting solenoid; b) quadruple magnets; c) a niobium sphere; and d) the quartz channel that holds the magnets and the sphere. Figure 3.1 is a drawing of these

parts put together.

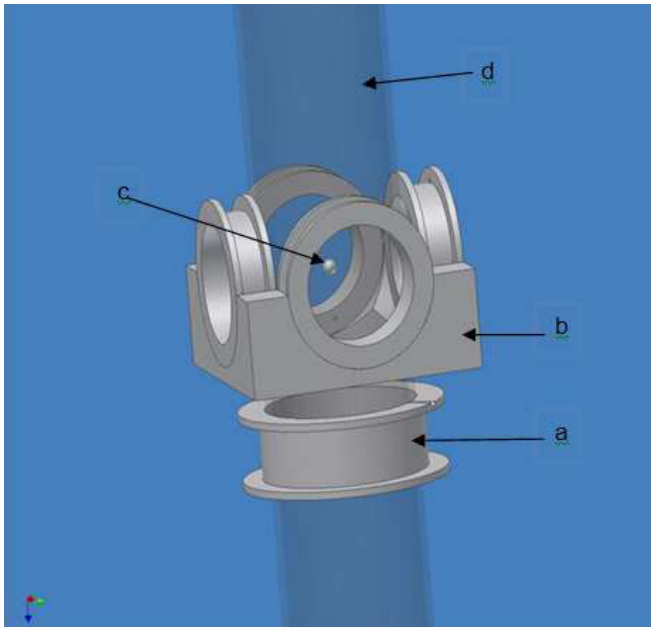


Figure 3.1: Schematic of magnetic trap with niobium sphere. The sphere, c, is lifted up by the launching solenoid, a, and centered and levitated by quadruple magnets, b.

## 3.1 Niobium Sphere

For this experiment a 3 mm ±0.005 mm niobium sphere is used as the object of levitation. It is made out of pure niobium and mass of 0.121 mg. Niobium has lower critical field of 0.25 T and a density of 8570 $kg/m^3$. The sphere was purchased from United States Ball Corp[13]. The reason for using niobium sphere is that it becomes superconducting at 9.2 K, well above liquid helium temperature, and its specific gravity is low enough that it can be levitated by a modest magnetic field.

| Diameter | Mass | $T_c$ | $B_{c1}$ |
|---|---|---|---|
| 3 mm ± 0.005 mm | 0.121 mg | 9.2 K | 0.25 T |

Table 3.1: Properties of niobium sphere

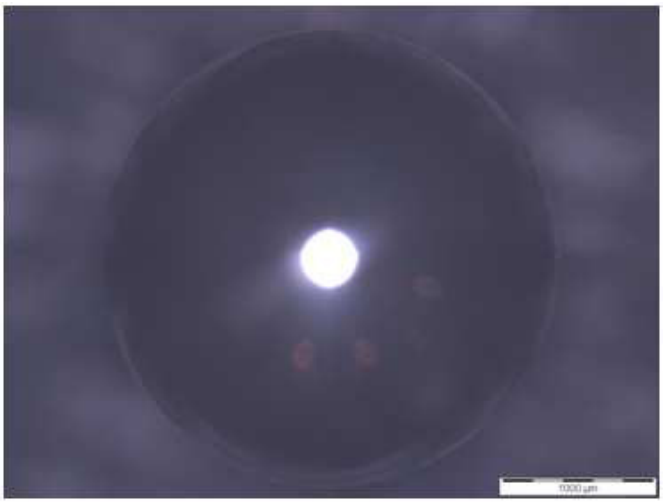

Figure 3.2: 3 mm niobium sphere

## 3.2 Launching Solenoid

Copper niobium titanium wires were used to build both the launching magnet and the quadruple magnet. The wire has critical temperature of 9.6 K, critical field of 8 T a diameter of 0.102 mm (insulated), contains 54 filaments, and it has critical current of approximately 6.8 A at 4.2 K. Three hundred meters of this wire was purchased from SUPERCON Inc most of which was used to build the magnets.

The launching solenoid's wire is wound around a cylindrical shaped aluminum mandrel. The solenoid has 1200 turns and with 3.15 A of current the maximum magnetic field at its center is 0.034 T. Since there are many more variables in designing such solenoids than there are equations or boundary conditions, the size determination of this solenoid can be obtained by several times running the calculations and guessing and correcting the length of solenoid, number of turns, inner and outer radii, maximum current applied, and size of the experimental apparatus. This experiment requires small sizes of magnets due to apparatus size limitations. The inner radius can be estimated by knowing the size of the channel, and outer radius is obtained by knowing the wire diameter, and estimating a filling factor of 70 %: The final design, inner radius of the launching solenoid is 12.1 mm and outer radius is 13.8 mm. To optimize the calculation of solenoid's parameters the length of solenoid was determined to be 8.0 mm. An image of final build of the launching solenoid is shown in

figure 3.3.

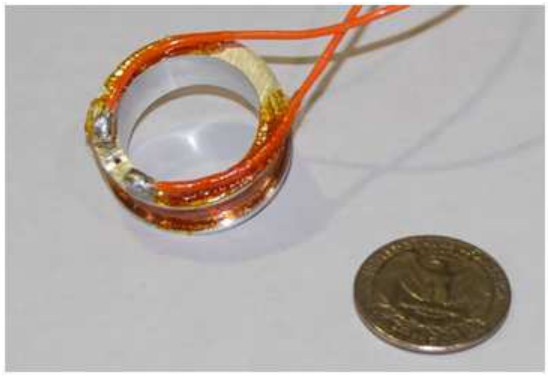

Figure 3.3: Solenoid consisting of 1200 turns of 0.102 mm diameter wire

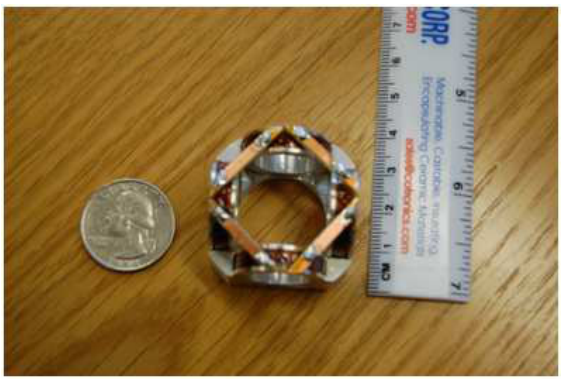

Figure 3.4: Quadruple magnet assembly

## 3.3 Quadruple Magnet

Each of the coils in the quadruple magnet is designed similarly to the launching solenoid, but with fewer turns and smaller diameter, since a smaller force is sufficient to stabilize the niobium sphere. Each coil of the quadruple magnet has 555 turn. The inner radius of each of the coils is 8.93 mm, outer radius is 10.6 mm, and length of each coil is 4.00 mm. The center of each coil is located 10.4 mm from the axis of the experiment. Figure 3.4 is an image of the quadruple magnet put together.

## 3.4 Optical Channel

Two different channels were used for the final assembly for the He II experiment. Channel 1 is an open channel consisting of a quartz tube of inner diameter of 20 mm and outer diameter of 22 mm that supports the magnets and also holds the sphere above the launching solenoid with a circular G-10 stopper. The size of the channel has been determined by requiring that it be at least four times the diameter of the sphere. In the present case the sphere is 3 mm in diameter; therefore, has minimal effect on the flow cross section as the inner diameter of the channel is 20 mm.

Channel 2 is an improved version built to allow experiments in helium gas or vacuum. This second new channel is a separate vessel that supports the magnets and is immersed

in the helium bath. It can be filled with helium by condensing helium gas from a separate gas bottle. This channel is also connected to a vacuum pump, so it is possible to control the amount of helium inside the experiment. This channel has a glass to metal seal that is leak-tight and it is connected to bellows and welded to a stainless steel tube that goes to outside room temperature. Figure 3.5 is a picture of the channel not connected to the experiment.

Figure 3.5: Glass channel is closed in the middle and has glass to metal seal at the top

## 3.5 Final Assembly & Data Acquisition

Once all the parts are ready, the assembly will be similar to figure 3.1, then the whole experimental apparatus is placed inside an optical cryostat. A high speed CCD camera and a light source are placed in front of the windows of the cryostat. Figure 3.6 is an image that shows the assembly from outside including the cryostat, the camera, lamp, vacuum pump, and all the plumping and wiring connections needed.

The main data obtained from the experiment are video images of the sphere oscillating in the magnetic trap. Aligned camera (X-Stream) captures the images and stores them on a computer. The software that is used to do that is called Motion Studio - Image Acquisition and processing from IDT (Integrated Design Tools). Then analysis of these videos is done in Matlab®. A more detailed description of this analysis is provided in a later section.

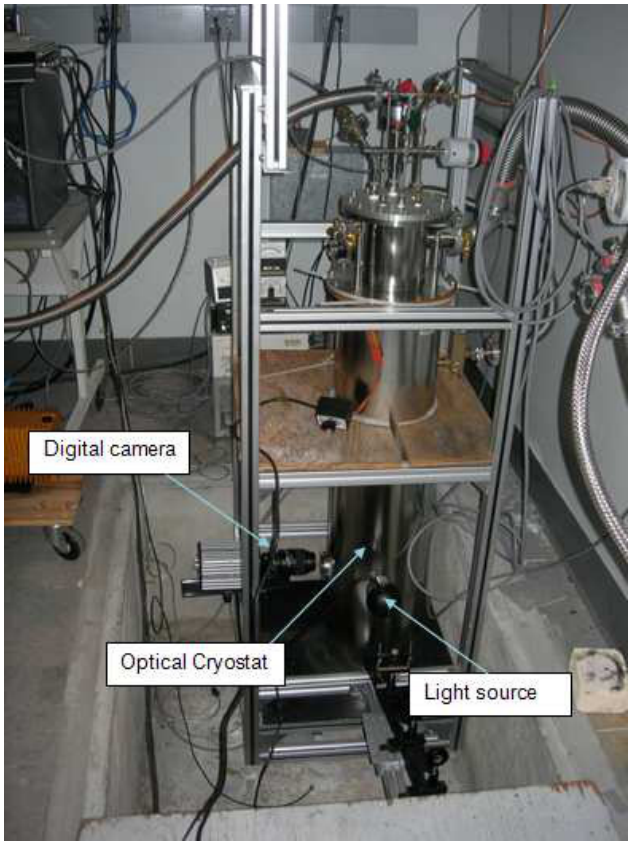


Figure 3.6: Outside image of the experiment that includes optical cryostat, high speed camera, light source, and other connections

# CHAPTER 4

# THEORY OF MEASUREMENT

## 4.1 Magnetic Forces

A few equations were used to predict the magnetic force of the magnets on the sphere as a function of location. Since the sphere is centered by the quadruples, it is always located on the axis of the channel and is parallel to radial component of the quadruples. Calculating magnetic field for such magnets is usually done using finite element analysis, but for our case due to the sphere oscillation and not being stable at only one location, it is a very difficult and cumbersome task to perform such calculations. Therefore, we have tried to use mathematical expansion formulas and Brown-Flax method to estimate the forces on the sphere. An exact formula exists to calculate the magnetic field at the center axis of a solenoid (on the axial axis). This equation is denoted by $B_0(z)$, the number zero denotes axis at the center of the solenoid, and is presented below as,

$$B_0(z) = \frac{\mu_0 * i * n}{2(r_o - r_i)} \left\{ (\frac{L_s}{2} + z) \ln \left[ \frac{\sqrt{r_o^2 + (\frac{L_s}{2} + z)^2} + r_o}{\sqrt{r_i^2 + (\frac{L_s}{2} + z)^2} + r_i} \right] \right. \\ \left. -(-\frac{L_s}{2} + z) \ln \left[ \frac{\sqrt{r_o^2 + (-\frac{L_s}{2} + z)^2} + r_o}{\sqrt{r_i^2 + (-\frac{L_s}{2} + z)^2} + r_i} \right] \right\} \tag{4.1}$$

where $\mu_0$ is permeability of free space and $\mu_0 = 4\pi \times 10^{-7}$ H/m , $i$ is applied current, $L_s$ is length of solenoid, $n$ is number of turns per length, $r_i$ is inner radius of solenoid, $r_o$ is outer radius of solenoid, and $z$ is some distance away from the center of the solenoid. Furthermore, we used the following equations developed by Dushkin[14] to calculate the radial and axial components of magnetic field of a solenoid at radii other than the center axis. The radial

component is used to calculate the force that the quadruple magnet applies to the sphere.

$$B_r(r,z) = -\frac{\mathrm{d}B_0(z)}{\mathrm{d}z}\frac{r}{2} + \frac{\mathrm{d}^3B_0(z)}{\mathrm{d}z^3}\frac{r^3}{16} \tag{4.2}$$

From the magnetic field equations, we are able to calculate the external forces acting on the sphere including forces due to buoyancy, and magnetic forces from both launching solenoid and quadruples. The force per unit volume due to gravity is given as,

$$F_g = (\rho_{sphere} - \rho_{He}) * g \tag{4.3}$$

and magnetic force per unit volume of launching solenoid is given as,

$$F_s(z) = \frac{1}{\mu_0}B_0(z)\frac{\mathrm{d}B_0(z)}{\mathrm{d}z} \tag{4.4}$$

and magnetic force per unit volume of the quadruple magnet is given as,

$$F_q(r) = \frac{16}{\mu_0}B_r(r,z_{const})\frac{\mathrm{d}B_r(r,z_{const})}{\mathrm{d}r} \tag{4.5}$$

where $\rho_{sphere}$ is the density of the sphere, and $\rho_{He}$ is the density of liquid helium, and $z_{const}$ is the distance that the center of each coil is located from the axis of the experiment and is 10.4 mm. It is also notable to mention that the numerical coefficient 16 in equation 4.5 comes from the fact that the radial component of the magnetic field and field gradient are made up of field component of each of four coils.

There are two sets of calculations to predict the behavior of niobium sphere and the forces that act upon it. These sets of calculations are based upon the two different methods of measuring drag, which were discussed in previous section, force flow and oscillation. So far, we have only completed experiments that use the oscillations as method of measuring drag and viscous forces; therefore, below we show some detail calculations related to the oscillation experiment; as future work, some calculations related to the force flow experiment is also presented at the last section which is entitled future work.

## 4.2 Oscillation experiment

We have developed a one dimensional equation to theoretically map the oscillation of the sphere. This equation is based on a more general one dimensional equation of motion for a sphere in a fluid obtained from Melling[15]. This equation was also used by Zhang[16] to

describe the motion of spherical particles in He II. Here we have used the same concept to describe the motion of the niobium sphere given as,

$$(\rho_{sphere} + \frac{\rho_{He}}{2})\frac{\mathrm{d}^2 z}{\mathrm{d}t^2} = -\frac{3C_d\rho_{sphere}}{4d_{sphere}}\frac{\mathrm{d}z}{dt}\left|\frac{\mathrm{d}z}{\mathrm{d}t}\right| - KF_M \tag{4.6}$$

where in our case the body force is made up of two components: the gravitational force plus radial magnetic force given as,

$$F_M = F_g + F_q \tag{4.7}$$

with $z$ being the direction that the sphere oscillates. $d_{sph}$ is sphere diameter and $F_M$ is sum of the magnetic and gravitational forces that is dependent on location of the sphere. $F_M$ and does not include the magnetic force of the launching magnet since it is not turned on during the oscillation. $K$ is an empirical force correction factor which in the present case is 2.25. $K$ is derived empirically first by comparing the frequency of the oscillation derived from calculations with frequency observed experimentally. To verify this correction factor, we have used finite element analysis field values obtained from Vector Fields® software to compare our theoretical calculations to predictions by the software. This $K$-factor corrects the force on the sphere, which is calculated by our equations, and it can also be verified by the software. Such a correction was expected due to lack of existence of a unique solution to the magnetic field equations. The value $K = 2.25$ has been very consistent throughout all the experiments, and it has shown to be a constant.

# CHAPTER 5

# EXPERIMENTAL PROCEDURE

First the experiment is cooled down to He II temperature. One great advantage of conducting visual experiments in He II is that it does not boil like He I at saturation pressure, so visualization is easier. Once temperature has reached 2.1 K, the lower magnet is turned on. Applying about 2 A of current to the bottom solenoid, this causes the sphere to rise up to near the center of the quadruple magnet. At this moment, the camera is turned on and adjusted to focus on the sphere. Then, the quadruple magnet is turned on to center the sphere. As described before this is one of major tasks of the quadruple magnet. The current in the quadruple is slowly ramped up to 3.15 A; this value is determined by calculating the restoring force needed to place the sphere in an equilibrium position. Once the niobium sphere is centered and reasonably stable the current to the bottom magnet is increased to 3.15 A, raising the sphere further up; This same position is maintained for all experiments for consistency reasons. When the sphere is stable, which only takes about few seconds, sphere oscillation is achieved by reducing the current to the bottom magnet to zero. This action causes the sphere to drop down to its lower equilibrium position and oscillate about this new equilibrium point. The damped oscillation is then recorded with the camera.

Data collected in this experiment is completely through high speed digital camera. Once the current to the bottom magnet is quickly decreased to zero, recording of the oscillation begins. One issue that arises during this data collection is the limitation of camera's memory. The data collection can take more than two minutes, and experimentally it was determined that the frequency of the oscillation is 10 to 10.5 Hz. Therefore, to collect more data over longer period of time, it was necessary to come up with a technique to record as much of data as possible to capture the decay time and behavior of the oscillation. To resolve this issue, we developed a technique that only captures segments of the oscillation with each

segment providing sufficient information about the velocity of the sphere. For the present set of experiments, we determined that to obtain enough data points, we only needed to capture about 0.5 seconds of the oscillation at 100 Hz, which gave us about 50 points of experimental data for each segment.

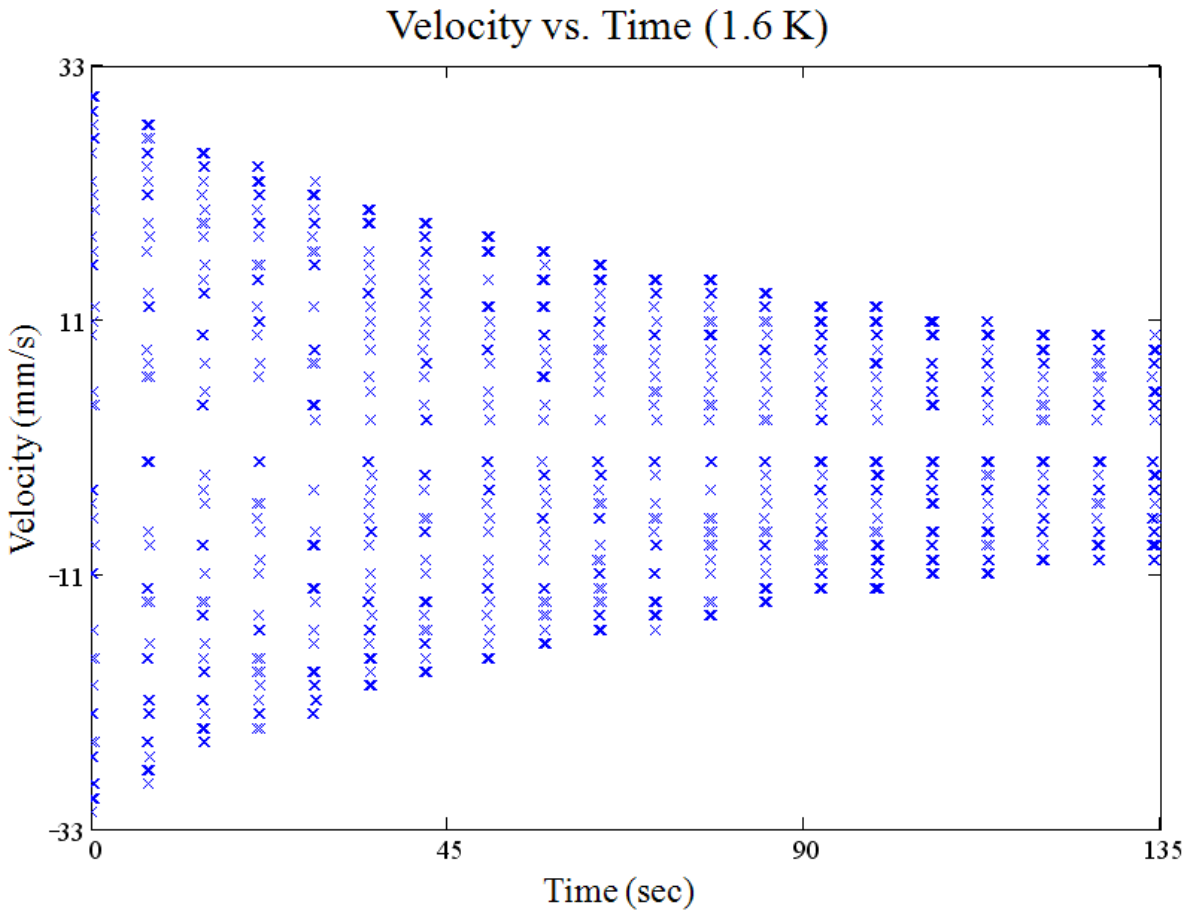


Figure 5.1: Velocity vs. time data collected at 1.6K

The image analysis of the data is done by cross correlation codes that we have written in Matlab®. A major part in this analysis is the recognition of the change in position of the sphere one image after another. Once cross-correlation is done between two images a graph can be obtained that provides information about how well the second image matches the first image after it has been moved by a certain number of pixels. This graph has a peak, which can be used to determine the distance the sphere has moved over a certain amount of time. Therefore, by using the known diameter of the sphere as a scale to convert pixels to

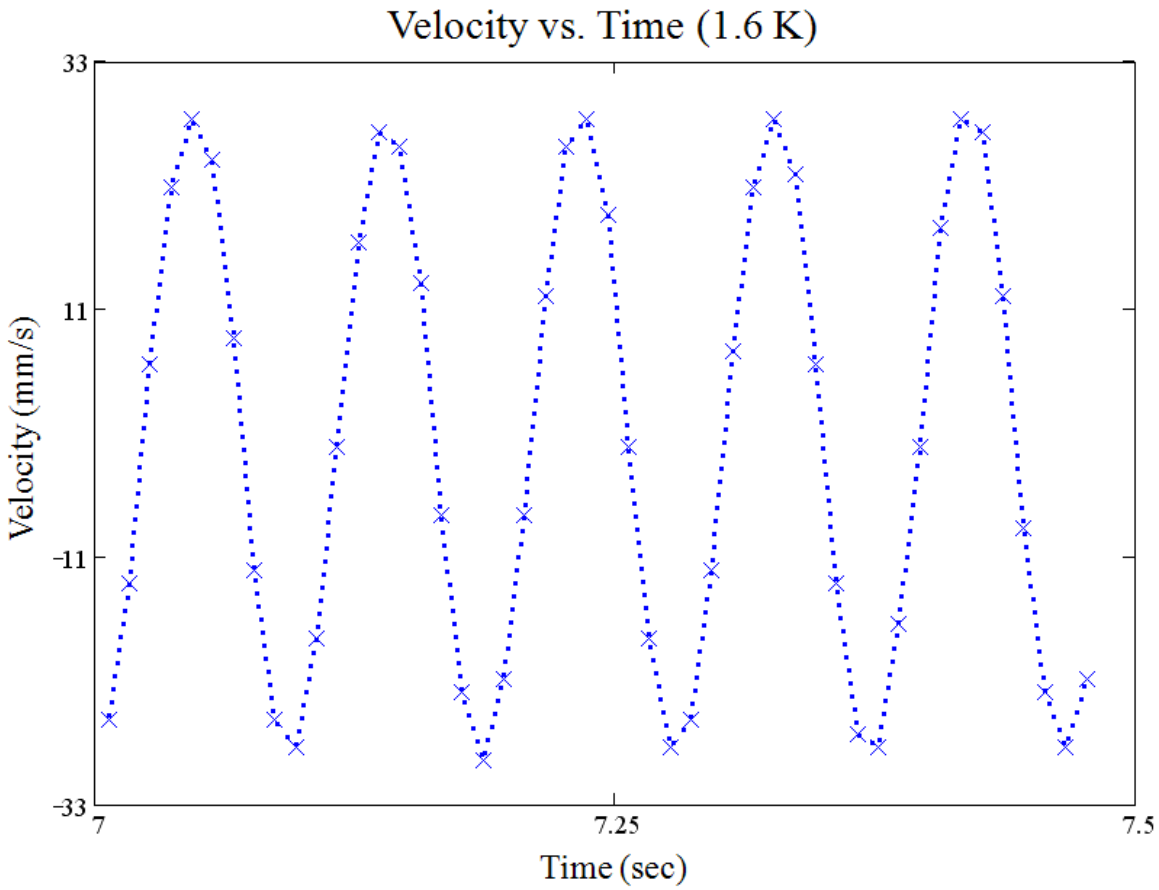


Figure 5.2: Close up of one segment of Figure 5.1 with 50 points in 0.5 seconds

metric units, and by knowing the frequency and number of frames, we can convert all those images to graphs similar to figure 5.1.

# CHAPTER 6

# RESULTS

Once all the images have been analyzed and converted to data, we can graph these points against the theoretical calculations and from there, estimate the drag coefficient by adjusting $C_d$ to best fit the theoretical curve. We have graphed both experimental velocities and velocities calculated in equation 4.6 versus time in figure 6.1. This graph only shows the first section of the data. We determine the drag coefficient for a certain Reynolds number by dividing the whole set of data into number of distinct pieces (usually 4 or 5). Then, we adjust the drag coefficient value for the theoretical calculations until a best fit is obtained. Changing the $C_D$ by more than $\pm 10$ % leads to an observable difference between experimental and theoretical curve. The velocity used to calculate the Reynolds number is based on the average maximum velocity amplitude over the segments that are used in the calculation.

From analyzing these data points we have created a graph of drag coefficient versus Reynolds number which is presented in figure 6.2. These data have been compared to similar measurements of $C_d$ obtained by measuring drag force on spheres moving through He II by Dowley, Firth and Hallett[12] in temperature range of 1.47 K to 2.13 K. Also, the line represents the $C_d$ in classical fluids.

To verify that the magnetic forces do not contribute directly to the damping of the sphere oscillation through eddy currents in the coil or coil form, we performed an experiment with the sphere suspended in vacuum. It should be noted that this experiment required some care since the sphere is insulated from the surrounding helium such that the light source easily can heat it above its critical temperature. In this experiment, the sphere oscillation amplitude did not noticeably decay within the duration of the measurement, which was about 200 s. Therefore, we have concluded that the magnetic forces impose no additional damping force on the sphere. This is shown in figure 6.3.

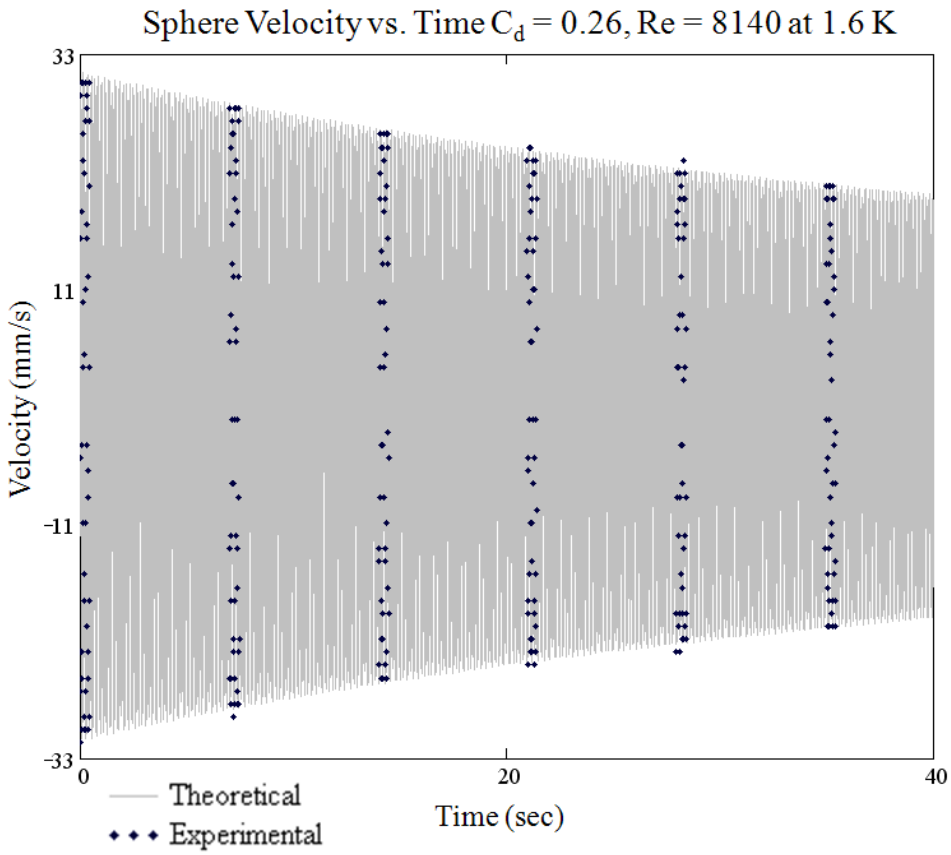


Figure 6.1: Drag coefficient determination by comparison of experimental data and theoretical data

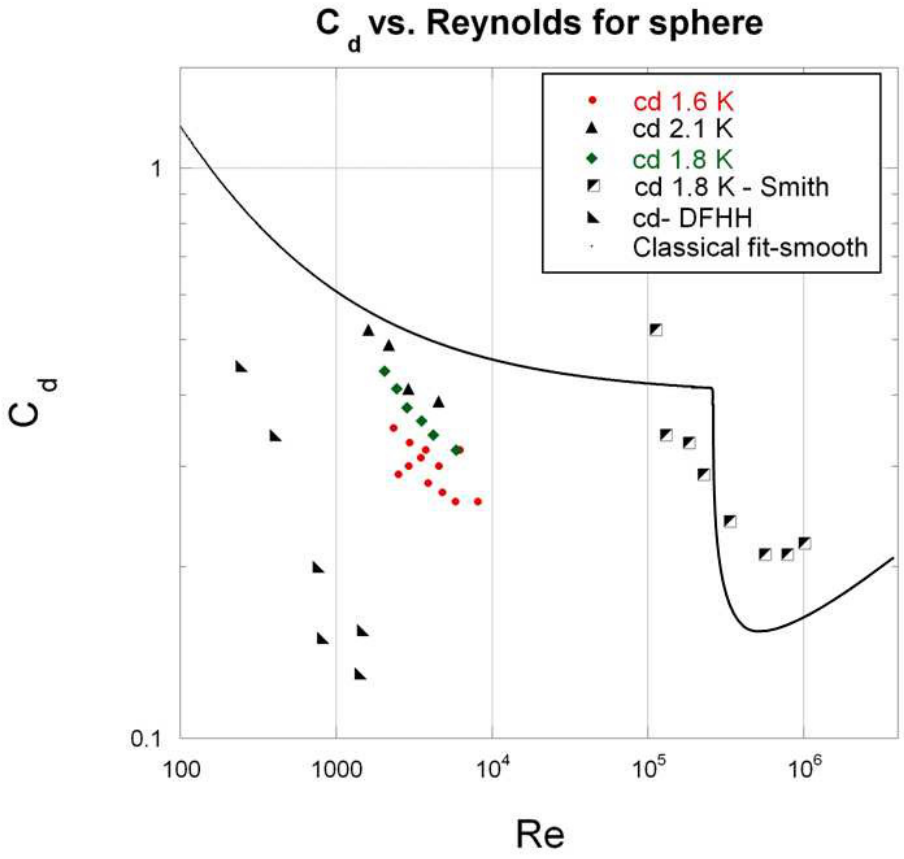


Figure 6.2: Comparison of $C_d$ vs. Reynolds number in He II and classical fluid. Also compared to DFHH, Dowley M W, Firth D R and Hollis Hallett[12] and Smith[7]

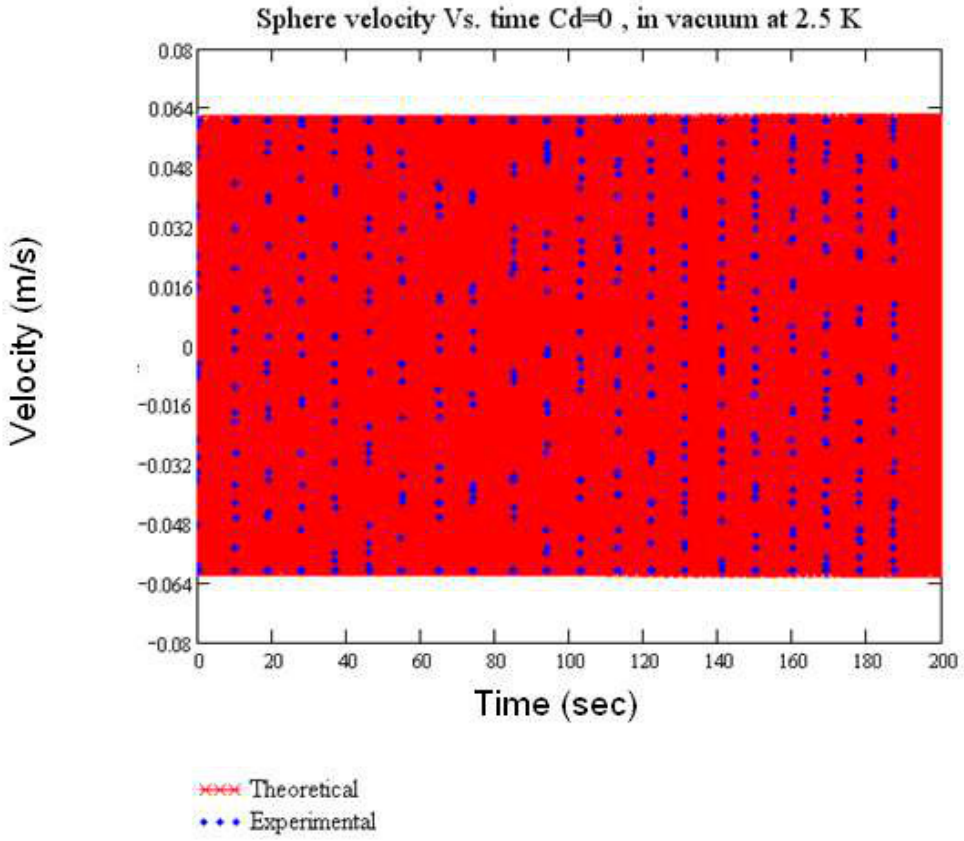


Figure 6.3: Oscillation in vacuum shows no damping

# CHAPTER 7

# CONCLUSION & DISCUSSION

A successful magnetic suspension system has been built, which is capable of suspending a perfectly diamagnetic sphere for visualization studies. Using this experiment we have measured the drag coefficient in He II in the range of Reynolds number 1000 to 10000. These results suggest that the drag coefficient in He II in the temperature range 2.1 K down to 1.6 K show values reasonably close to classical measurements. Furthermore, the data suggest that there may be small temperature dependence in the drag coefficient measurements. However, additional measurements are required to confirm this observation.

By performing this experiment in He I and helium gas, we can verify that our system produces classical values for the drag coefficient. So far, we have performed experiments in vacuum to show that the damping seen in the oscillation is only due to the drag force on the sphere from the fluid, and the sphere moving up and down does not change the magnetic field enough for it to affect the drag force.

Unfortunately, we have encountered a very common problem while performing this experiment in vacuum. Due to radiation heating of the sphere and absence of any medium to keep the sphere cool, it warms up and drops. Once this happens, we cannot run the experiment anymore because the sphere is not perfectly diamagnetic anymore and has flux trapped in it. So the only solution is to warm up the experimental space and boil off all the liquid helium.

# CHAPTER 8

# FUTURE WORK

## 8.1 Different Spheres

We need to perform this oscillation experiment with different size spheres to verify our observations, and further research into oscillation past spheres to determine critical Keulegan-Carpenter number, which has not been verified yet, especially for superfluid helium. Moreover, our experiment needs to cover much larger range of Reynolds numbers, so we need to implement ways to do experiments in drag crisis regime and Stokes' regime.

Using different diameter spheres can change the range of Reynolds numbers that we have already covered. This change can bring about a change in frequency. Although a smaller diameter sphere might be desirable for future work, it could prove to be rather less stabile in high Reynolds number regime. We have estimated that by using smaller diameter spheres decay time will not change very much, so a change in diameter might not prove worthy. On the other hand, using a different material can be a better choice. It is important for the material to be perfectly diamagnetic in He II, and be light enough so it would be levitated by the magnets. Some of these materials that are worth looking further into would be lead, tantalum, tin, and possibly more.

## 8.2 Force flow experiment

As it was mentioned before, another method to measure drag is to do it in a steady manner. Steady drag measurement can be possible in a force flow experiment, hence only the final distance that the sphere moves is of interest. Moreover, in force flow experiment we do not need to worry about an exact solution to the magnetic field equations. The field values can be approximated closely by numerical solutions. Nevertheless, we have some expected results that we can obtain from a force flow experiment, and whether it is feasible to do with

our current system. In force flow experiment an actuator and a bellow is used to introduce a constant velocity to the flow depending on the area of the channel and the area of the bellow. We have calculated the maximum velocity that can be introduced based on the current apparatus setup that we have. Our current stepper motor with linear stroke can output maximum velocity of 0.0254 m/s which for the area of the channel that we use can reach 1.5 m/s.

Since the method to calculate the drag force on the sphere is to measure the displacement of the sphere after the flow has been established in the channel, we must record the displacement by using a camera. However, before running the actual experiment we must determine whether the displacement is enough for the camera to be detectable.

We do this by calculating the drag force by using equation 1.1. Where velocity, $v$, is replaced with maximum velocitym $v_{max}$. From equation 4.7, we write a force equation that has the force of the launching solenoid added to the total force assuming that it will stay turned on during the experiment.

The new total force per unit volume is given as,

$$F_{M2} = K(F_g + F_q) + F_s \tag{8.1}$$

where K is the correction factor that corrects the gravitational plus radial component and is discussed previously. K does not apply to the solenoid since there exists exact solution to calculate that force. We use steady force analysis to set the drag force and gravitational plus magnetic forces equal to each other to find the final location at which the sphere becomes stable and is given as,

$$F_{M2} = F_D \tag{8.2}$$

All these equations have been set to have one independent variable while at the center axis of the channel. The above equation is only dependent on one variable and can be solved for that one variable to produce the final location of the sphere. These calculations have been done in Mathcad® using a trial and error solve block. The result is that the sphere shall move a distance of 1.6 mm from its original position at fluid velocity $v = v_{max}$. This is almost the radius of the current sphere used and can be easily detected by our visualization equipment. We have assumed a drag coefficient, $C_d$, of 0.45 for this calculation. The actual drag may be different, and will be determined by experiment.

In an experiment, the flow stops after a few seconds. The sphere will not only move immediately to the new location, but it will oscillate around that new equilibrium point until it comes to rest. Therefore, we must determine how long after the desired velocity has been reached the sphere comes to its stop location. This timing is very important because the duration of stroke in the experiment is about 6.3 seconds at maximum velocity. This means that there is only six seconds after the initiation of the linear actuator that we have time to record the final position of the sphere. To predict the oscillation of the sphere, we have used equation 4.6, where $F_{M2}$ is the magnetic and gravitational force on the sphere at some $z$ location and replaces $F_M$. To obtain numerical solution we have used Runge-Kutta-Nystrom method. Another method to solve this equation is to expand the force equation to a polynomial and solve it using Runge-Kutta method, which can speed up the process by a lot. The result is shown in figure 8.1.

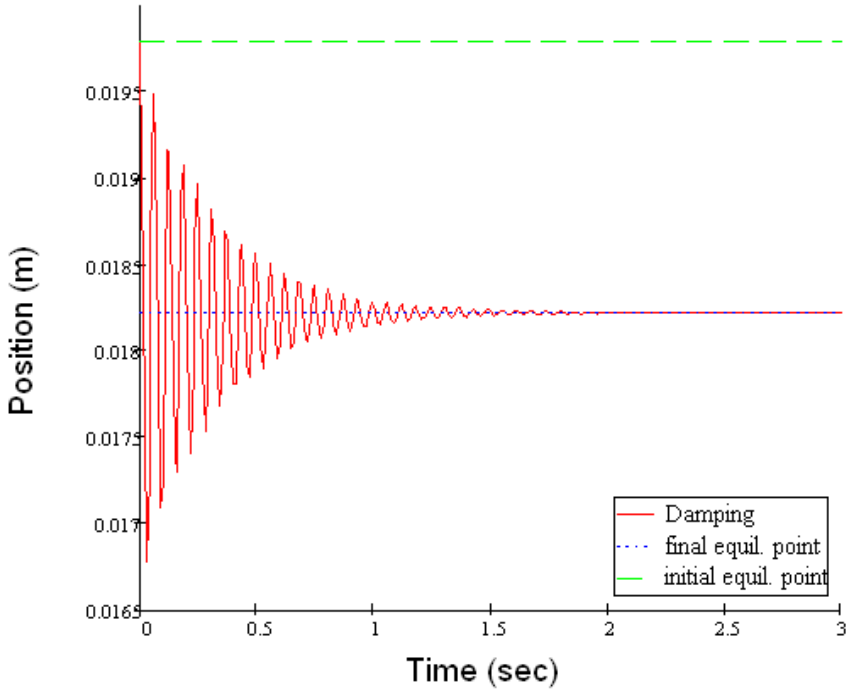


Figure 8.1: Position vs. time calculation for the sphere in force flow with maximum velocity

From figure 8.1, we can see that the sphere will come to a resting point in 1.5 seconds. Therefore, we shall be able to detect the sphere's final position in time.

# CHAPTER 9

# SUMMARY

Study of thermodynamics and physical properties of He II have been an interest of many scientists since its discovery. In addition, the study of drag force, specifically, on a sphere has been an interest for many years. We have known that drag force is dependent upon the shape of the object, fluid velocity and density. In most commonly known fluids, this property has been well studied. A drag coefficient, which is very important in determining the drag force, has been calculated for many different shapes with respect to fluid velocity. A sphere is a shape that has been studied in depth and can produce a drag coefficient that can be well predicted, specifically in laminar regimes.

Since the discovery of He II, there has not been much study related to the measurement of drag on a sphere. There is an interest in developing systems that can measure drag on a sphere from laminar to turbulent regimes and to compare these values to classical values. We believe that we have devised such a system that can be used not only to study drag forces on a sphere in He II, but also to study oscillation of a sphere in He II. Study of oscillation is a field that focuses more on transient and more dynamic aspect of fluids and how they behave. This area of study has not been fully developed, not even in classical fluids.

We have been able to visualize an oscillating sphere and from that we have extracted drag coefficient and velocity information. In addition, we have shown the possibility for our system to be revised, so lower and higher Reynolds numbers can be achieved. Also, a steady drag measurement system can be used to measure drag coefficient, which involve less systematic error.

# REFERENCES


[1] Frank M. White, *Fluid Mechanics*, 4th ed. (Mcgraw-Hill College, 1998), 457. 1.1

[2] R. J. Donnelly, "Cryogenic fluid dynamics," *Journal of Physics Condensed Matter*11 (1999): 7783-7834. 1.1

[3] Hermann Schlichting, *Boundary Layer Theory*, 7th ed. (McGraw-Hill Science/Engineering/Math, 1979) 1.1

[4] Frank M. White, *Viscous Fluid Flow*, 1st ed. (McGraw-Hill, 1991), 182. 1.1

[5] S. W. Van Sciver, *Helium cryogenics*, 1st ed. (Plenum Pub Corp, 1986), 101. 1.2.1

[6] E. J. Yarmchuk and R. E. Packard, "Photographic studies of quantized vortex lines," *Journal of Low Temperature Physics*46, no. 5 (1982): 479-515. 1.2.2

[7] M. R. Smith and S. W. Van Sciver, "Measurement of the pressure distribution and drag on a sphere in flowing helium I and helium II," *Advances in cryogenic engineering 43*(1998): 1473-1479. 2, 2.1, 6.2

[8] R. A. Laing and H. E. Rorschach Jr, "Hydrodynamic Drag on Spheres Moving in Liquid Helium," Physics of Fluids 4 (1961): 564. 2, 2.2

[9] L D Landau and E.M. Lifshitz, *Fluid Mechanics, Second Edition: Volume 6*, 2nd ed. (Butterworth-Heinemann, 1987). Page 90 2

[10] M. Niemetz and W. Schoepe, "Stability of Laminar and Turbulent Flow of Superfluid 4 He at mK Temperatures Around an Oscillating Microsphere," Journal of Low Temperature Physics 135, no. 5 (2004): 447-469. 2, 2.3

[11] M.R. Smith, Y.M. Eyssa, and S.W. Van Scivrr, "Design of a superconducting magnetic suspension system for a liquid helium flow experiment," *Applied Superconductivity, IEEE Transactions on 7*, no. 2 (1997): 382-385, doi:10.1109/77.614509. 2

[12] Dowley M W, Firth D R and Hollis Hallett A C 1961 *Proc. 7th Int. Conf. on Low Temperature Physics*2, 6, 6.2

[13] "Steel Precision Balls Custom Applications, California," http://www.usball.com/balls/default.html. 3.1

[14] C. Dushkin et al., "Magnetic field in a thick superconducting solenoid for dynamic levitation of objects," *Journal of Applied Physics 91*, no. 12 (2002): 10212-10214. 4.1

[15] A. Melling, "Tracer particles and seeding for particle image velocimetry," *Measurement Science and Technology 8*, no. 12 (1997): 1406-1416. 4.2

[16] T. Zhang, D. Celik, and S. W. Van Sciver, "Tracer Particles for Application to PIV Studies of Liquid Helium," *Journal of Low Temperature Physics 134*, no. 3 (February 1, 2004): 985-1000, doi:10.1023/B:JOLT.0000013213.61721.51. 4.2

# BIOGRAPHICAL SKETCH

**ALI HEMMATI**

**Major:**

Mechanical Engineering

**Awards & Honors:**

-Florida State University Teaching Fellowship (2007)

-Florida State University Scholarship (2004-2007)

-Florida Bright Futures Scholarship (2004-2007)

-President's List at Florida State University (spring 2005), and Dean's list (Fall 2005, Spring 2006, Fall 2006, Spring 2007)

-Pi Tau Sigma Mechanical Engineering Honor Society, Golden Key International Honour Society, Pi Mu Epsilon National Mathematics Honor Society